Acta Crystallographica Section B
**Structural Science**
ISSN 0108-7681

# Monitoring structural transformations in crystals. 11. Yang photocyclizations – one type of reaction, but diversity of structural changes

**Ilona Turowska-Tyrk,[a]* Julia Bąkowicz[a] and John R. Scheffer[b]**

[a]Department of Chemistry, Wrocław University of Technology, Wybrzeże Wyspiańskiego 27, 50-370 Wrocław, Poland, and [b]Department of Chemistry, University of British Columbia, 6174 University Blvd, Vancouver, British Columbia, Canada V6T 1Z3

Correspondence e-mail: ilona.turowska-tyrk@pwr.wroc.pl

Received 11 July 2007
Accepted 17 October 2007

For Part 10 see Turowska-Tyrk *et al.* (2007).

Structural changes proceeding in a crystal during the Yang photocyclization of the salt 6,6-diethyl-5-oxo-5,6,7,8-tetrahydronaphthalene-2-carboxylate with (1*S*)-1-(4-methylphenyl)-ethylamine were monitored by means of X-ray structure analysis. The course of the photoreaction was evaluated on the basis of the geometrical parameters for the pure reactant crystal. Variations in the cell constants, the product content, the geometry of the reaction centre, the orientation of molecular fragments and the geometry of hydrogen bonds were described and analyzed. It was found that the cell volume increased until 56% product content and decreased thereafter. The distance between the directly reacting C atoms was constant, $\sim 3.0$ Å, until $\sim 75\%$ reaction progress. Analysis of the distance between atoms that would participate in the formation of the second (unobserved) enantiomorph excluded the formation of such an isomer. Molecular fragments varied their orientation during the photoreaction, and the largest change was observed for the carboxylate group despite its participation in strong hydrogen bonds. The geometry of the hydrogen bonds changed during the photoreaction. The largest change was 0.17 Å for the $D\cdots A$ distance and 13° for the $D$—H$\cdots A$ angle. A comparison of the intra- and intermolecular parameters for the studied salt with data for other compounds undergoing the Yang photocyclization in crystals revealed a diversity of structural changes brought about by this type of photochemical reaction.

## 1. Introduction

Photochemical reactions proceeding in the solid state, especially in crystals, have been the subject of wide interest. The reasons for the importance of such reactions are of a practical and theoretical nature (Boldyreva, 1999; Cohen & Schmidt, 1964; Ohashi, 1988, 1993, 1998; Ramamurthy, 1991; Schmidt, 1971; Tanaka, 2003). Photoreactions conducted in the solid state are often highly selective and provide pure products which are impossible to obtain in the solution state. They are environmentally friendly because they do not require the use of solvents. They have also been applied to modern technologies (Balzani, 2003; Dürr & Bouas-Laurent, 1990; Irie, 2000). Photochemical reactions in crystals have been examined by many techniques (Boldyreva, 1999), one of the most powerful being X-ray structure analysis. In recent years several papers have appeared on monitoring structural changes during transformations from pure reactant crystals towards pure product crystals (Fernandes & Levendis, 2004; Ohba & Ito, 2003; Turowska-Tyrk, 2001, 2003, 2004; Turowska-Tyrk & Trzop, 2003; Turowska-Tyrk, Bąkowicz, Scheffer & Xia, 2006; Turowska-Tyrk *et al.*, 2006*a*). Studies of this type require data

collections and structure determinations for many partly reacted crystals, *i.e.* those containing different amounts of reactant and product. This may be one of the reasons why they have been undertaken rather rarely. We believe that this will change in the future (Turowska-Tyrk *et al.*, 2006*b*), since such studies provide valuable information. Knowledge of crystal structures for partly reacted crystals gives detailed information about the course of a reaction in a crystal. For instance, it helped to understand the formation of two enantiomorphs in crystals, although the formation of only one enantiomorph was predicted on the basis of the structure of a pure reactant crystal (Turowska-Tyrk, Bąkowicz, Scheffer & Xia, 2006; Turowska-Tyrk *et al.*, 2007).

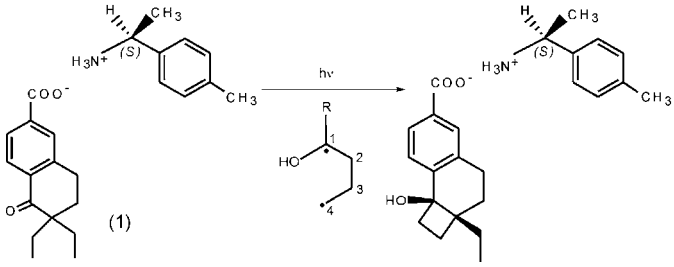


In this paper we will present the results of monitoring the Yang photocyclization of the 6,6-diethyl-5-oxo-5,6,7,8-tetrahydronaphthalene-2-carboxylate salt with (1*S*)-1-(4-methylphenyl)ethylamine (1). The reaction is presented above. The mechanism of the Yang photocyclization consists of two steps (Chen *et al.*, 2004; Yang *et al.*, 2005*a*,*b*). In the first step a $\gamma$-H atom is abstracted and transferred to the O atom of a carbonyl group and, as a result, a 1,4-hydroxybiradical is formed (shown below the arrow in the above scheme). In the second step a cyclobutane ring is created from the 1,4-hydroxybiradical. The solid-state Yang photocyclization has been previously monitored for the 1-(4-carboxybenzoyl)-1-methyladamantane salt with (*R*)-(+)-1-phenylethylamine (2), and the 2-(4-carboxybenzoyl)-2-methyl-*endo*-bicyclo[2.1.1]hexyl salt with (*S*)-(−)-1-phenylethylamine (3) (Turowska-Tyrk, Bąkowicz, Scheffer & Xia, 2006; Turowska-Tyrk *et al.*, 2007).

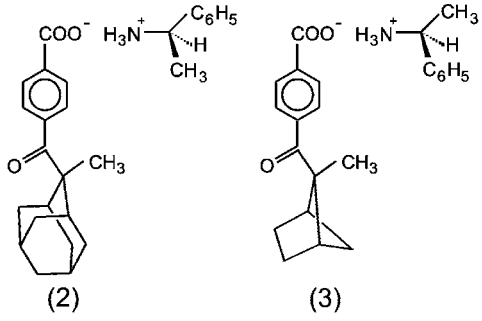


## 2. Experimental

The experiments were conducted on one crystal of (1). They followed preliminary experiments, which were undertaken in order to estimate the optimum conditions of the photoreaction, *i.e.* time of irradiation and beam wavelengths. All irradiation and diffraction experiments were conducted in a dark room. The crystal was irradiated in steps using an Hg 100 W lamp and a WG-320 glass filter. The filter blocked shorter and transmitted longer wavelengths: 0% transmittance for $\lambda <$ 300 nm, about 95% transmittance for $\lambda$ = 350 nm and 100% transmittance for $\lambda >$ 365 nm. The transmitted beam contained wavelengths characteristic of the low-energy tail of the $n,\pi^*$ absorption spectrum (Enkelman *et al.*, 1993; Novak *et al.*, 1993*a*,*b*) of (1). The direction of the beam was perpendicular to the longest crystal edge. The crystal was rotated during irradiation. The low energy of the beam, the perpendicular direction of the irradiation, the rotation of the crystal during irradiation and the thinness of the crystal ensured good penetration of the object by UV–vis radiation, and the homogeneity of the photoreaction. The length of time for each irradiation was as follows: 0, 10, 30, 60, 90, 120, 150, 180, 240, 300 and 360 min.

After each irradiation step, X-ray data were collected. The reflections were collected by means of a CCD diffractometer. The general strategy for data collection using area-detector diffractometers was described by Scheidt & Turowska-Tyrk (1994). The cell constants for each data collection were determined on the basis of the 1000 strongest reflections (Oxford Diffraction, 2003). No problems were encountered during the determinations of the cell constants. For all stages of the photoreaction, including the pure reactant and pure product crystals, the number of reflections for which the positions were predicted well by the orientation matrix was almost constant: 99.7% in the case of the pure product crystal and 94.1% for the pure reactant crystal. This indicates that the photoreaction occurred homogenously, *i.e.* there were no macroscopic regions of separated reactant and product during the photoreaction.

The intensities of the reflections were corrected for Lorentz and polarization effects (Oxford Diffraction, 2003). The structure determination was completed for 0, 10, 30, 60 and 300 min of crystal irradiation, *i.e.* for 0, 28.6, 56.5, 72.6 and 100% of the product in the crystal. The percentage of the product in the crystal was determined during the structure refinements. For irradiation times 90, 120, 150, 180, 240 and 360 min the quality of the structures was not satisfactory and data for them are not presented in this paper. The structures were solved by means of *SHELXS*97 (Sheldrick, 1990) and refined using *SHELXL*97 (Sheldrick, 1997). The absolute structure was assigned on the basis of the known absolute configuration of the (1*S*)-1-(4-methylphenyl)ethyl ammonium cation. In the case of the pure reactant and pure product crystals, all non-H atoms were refined anisotropically and all H atoms were refined isotropically with constraints. For the partly reacted crystals, for which the reactant was the major component, initial atomic coordinates were taken from the pure reactant crystal. For the partly reacted crystals, for which the product was the major component, initial atomic coordinates were taken from the pure product crystal. In both cases the first atoms of the minor component were found in difference-Fourier maps and the remaining atoms were located geometrically. For the partly reacted crystals, the major component was refined anisotropically and the minor

**Table 1**
Experimental details.

| | 0.0%P | 28.6%P | 56.5%P | 72.6%P | 100%P |
|---|---|---|---|---|---|
| Crystal data | | | | | |
| Chemical formula | $C_{24}H_{31}NO_3$ | $C_{24}H_{31}NO_3$ | $C_{24}H_{31}NO_3$ | $C_{24}H_{31}NO_3$ | $C_{24}H_{31}NO_3$ |
| $M_r$ | 381.50 | 381.50 | 381.50 | 381.50 | 381.50 |
| Cell setting, space group | Orthorhombic, $P2_12_12_1$ | Orthorhombic, $P2_12_12_1$ | Orthorhombic, $P2_12_12_1$ | Orthorhombic, $P2_12_12_1$ | Orthorhombic, $P2_12_12_1$ |
| Temperature (K) | 299 (2) | 299 (2) | 299 (2) | 299 (2) | 299 (2) |
| $a, b, c$ (Å) | 6.7448 (18), 11.849 (3), 26.976 (6) | 6.7891 (12), 11.852 (2), 26.822 (5) | 6.8320 (7), 11.8970 (15), 26.609 (3) | 6.8632 (8), 11.9445 (17), 26.305 (4) | 6.8834 (7), 12.0641 (15), 25.924 (3) |
| $V$ (Å $^3$) | 2155.9 (9) | 2158.2 (7) | 2162.8 (4) | 2156.4 (5) | 2152.8 (4) |
| $Z$ | 4 | 4 | 4 | 4 | 4 |
| $D_x$ (Mg m$^{-3}$) | 1.175 | 1.174 | 1.172 | 1.175 | 1.177 |
| Radiation type | Mo $K\alpha$ | Mo $K\alpha$ | Mo $K\alpha$ | Mo $K\alpha$ | Mo $K\alpha$ |
| $\mu$ (mm$^{-1}$) | 0.08 | 0.08 | 0.08 | 0.08 | 0.08 |
| Crystal form, colour | Block, colourless | Block, colourless | Block, colourless | Block, colourless | Block, colourless |
| Crystal size (mm) | 0.40 × 0.30 × 0.25 | 0.40 × 0.30 × 0.25 | 0.40 × 0.30 × 0.25 | 0.40 × 0.30 × 0.25 | 0.40 × 0.30 × 0.25 |
| Data collection | | | | | |
| Diffractometer | Kuma KM4CCD | Kuma KM4CCD | Kuma KM4CCD | Kuma KM4CCD | Kuma KM4CCD |
| Data collection method | $\omega$ scans | $\omega$ scans | $\omega$ scans | $\omega$ scans | $\omega$ scans |
| Absorption correction | None | None | None | None | None |
| No. of measured, independent and observed reflections | 11 662, 3696, 2324 | 11 658, 3750, 1914 | 11 741, 3780, 1869 | 11 703, 3760, 1767 | 11 650, 3741, 1344 |
| Criterion for observed reflections | $I > 2\sigma(I)$ | $I > 2\sigma(I)$ | $I > 2\sigma(I)$ | $I > 2\sigma(I)$ | $I > 2\sigma(I)$ |
| $R_{int}$ | 0.053 | 0.061 | 0.065 | 0.067 | 0.096 |
| $\theta_{max}$ (°) | 25.0 | 25.0 | 25.0 | 25.0 | 25.0 |
| Refinement | | | | | |
| Refinement on | $F^2$ | $F^2$ | $F^2$ | $F^2$ | $F^2$ |
| $R[F^2 > 2\sigma(F^2)]$, $wR(F^2)$, $S$ | 0.062, 0.194, 1.00 | 0.059, 0.175, 0.91 | 0.067, 0.203, 0.96 | 0.068, 0.212, 0.96 | 0.061, 0.181, 0.84 |
| No. of reflections | 3696 | 3750 | 3780 | 3760 | 3741 |
| No. of parameters | 255 | 327 | 327 | 327 | 254 |
| H-atom treatment | Constrained to parent site | Constrained to parent site | Constrained to parent site | Constrained to parent site | Constrained to parent site |
| Weighting scheme | $w = 1/[\sigma^2(F_o^2) + (0.121P)^2]$, where $P = (F_o^2 + 2F_c^2)/3$ | $w = 1/[\sigma^2(F_o^2) + (0.0993P)^2]$, where $P = (F_o^2 + 2F_c^2)/3$ | $w = 1/[\sigma^2(F_o^2) + (0.108P)^2]$, where $P = (F_o^2 + 2F_c^2)/3$ | $w = 1/[\sigma^2(F_o^2) + (0.1113P)^2]$, where $P = (F_o^2 + 2F_c^2)/3$ | $w = 1/[\sigma^2(F_o^2) + (0.0813P)^2]$, where $P = (F_o^2 + 2F_c^2)/3$ |
| $(\Delta/\sigma)_{max}$ | < 0.0001 | < 0.0001 | < 0.0001 | < 0.0001 | < 0.0001 |
| $\Delta\rho_{max}$, $\Delta\rho_{min}$ (e Å$^{-3}$) | 0.37, −0.20 | 0.20, −0.17 | 0.21, −0.18 | 0.16, −0.15 | 0.16, −0.18 |
| Extinction method | *SHELXL* | *SHELXL* | *SHELXL* | *SHELXL* | None |
| Extinction coefficient | 0.025 (5) | 0.019 (3) | 0.027 (5) | 0.037 (6) | – |
| Absolute structure | Based on known absolute configuration of the cation | Based on known absolute configuration of the cation | Based on known absolute configuration of the cation | Based on known absolute configuration of the cation | Based on known absolute configuration of the cation |

Computer programs used: *CrysAlis* (Oxford Diffraction, 2003), *SHELXS*97 (Sheldrick, 1990), *SHELXL*97 (Sheldrick, 1997), *ORTEP*3 *for Windows* (Farrugia, 1997).

component isotropically; the positions of the H atoms were found geometrically and refined with constraints. The H atom in the OH group was omitted. In the case of the partly reacted crystals, the methylphenyl group of the organic cation was refined with constraints; the geometry of this group was taken from the crystal of the pure product. Owing to a reactant–product disorder, which is always a feature of partly reacted crystals, the use of constraints and restraints for geometrical and thermal parameters was necessary. The following instructions from *SHELXL*97 (Sheldrick, 1997) were applied: AFIX, DFIX, DANG, FLAT and SIMU. Selected experimental data for the reported structures are given in Table 1.

In order to check if the photoreaction of (1) stops in the absence of UV–vis radiation, an additional data collection was carried out 1 d after the data collection for one partly reacted crystal. The product content, determined during the structure refinement, was statistically the same for both cases: the difference was smaller than one standard deviation. This structure determination also showed that the photoreaction of (1) was not influenced by X-rays.

## 3. Results and discussion

Fig. 1 presents an *ORTEP* view of a reactant molecule of (1) in the pure reactant crystal, a product molecule in the pure product crystal and the reactant superimposed on the product in the partly reacted crystal. As can be seen, the overall shape of the product and reactant molecules is very similar. This is the reason why crystals did not crack during the photochemical reaction studied, *i.e.* the reaction proceeded in a

**Table 2**
Values of geometrical parameters describing the Yang photocyclization.

| | $d$ (Å) | $D$ (Å) | $\omega$ (°) | $\Delta$ (°) | $\theta$ (°) |
|---|---|---|---|---|---|
| Ideal value | < 2.7 | | 0 | 90–120 | 180 |
| Average literature value† | 2.64 (8) | < 3.00 (9) | 54 (10) | 82 (8) | 116 (3) |
| Compound (1) | 2.77 | 3.023 | 67.5 | 74.1 | 112.6 |

† The mean values of $d$, $\omega$, $\Delta$ and $\theta$ are given for 54 aromatic ketones undergoing the Yang photocyclization (Natarajan *et al.*, 2005) and $D$ for 53 structures (Xia *et al.*, 2005).

single-crystal-to single-crystal manner (Cohen, 1975*a*,*b*; Lavy *et al.*, 2004; Weiss *et al.*, 1993). This property enabled the photoreaction to be monitored by means of X-ray structure analysis.

### 3.1. Geometrical demands for the Yang photocyclization in crystals

The Yang photocyclization proceeds in crystals only when special geometrical conditions are fulfilled (Ihmels & Scheffer, 1999; Natarajan *et al.*, 2005). The scheme below presents the geometrical parameters used to describe such conditions. Table 2 gives values for these parameters for (1). Additionally, the table contains the mean values for over 50 aromatic ketones undergoing the Yang photocyclization, and the ideal values (Natarajan *et al.*, 2005; Xia *et al.*, 2005). The ideal value for the distance between the carbonyl O atom and the $\gamma$-H atom, $d$, is smaller than 2.7 Å, *i.e.* smaller than the sum of the van der Waals radii (Ihmels & Scheffer, 1999; Natarajan *et al.*, 2005). Nevertheless, there are exceptions to the above relationship, *e.g.* the Yang photocyclization for a compound in which $d$ in a pure reactant crystal was 3.09 Å (Cheung *et al.*, 1999). The formation of a cyclobutane ring also requires that the distance between directly reacting C atoms, $D$, is not too long. According to this, the Yang photocyclization was not observed in crystals where $D$ was greater than 3.20 Å (Xia *et al.*, 2005). The observed mean value of $D$ is 3.00 (9) Å (Xia *et al.*, 2005). As can be seen from Table 2, in the case of (1) the values of the geometrical parameters for the pure reactant crystal are close to the average values. This indicates that (1) should undergo the Yang photocyclization in the crystalline state. It should be added that a molecule of (1) has six $\gamma$-H atoms, but only one of them can take part in the Yang photocyclization. The $d$ parameter for only one H atom has a value close to 2.7 Å, namely 2.77 Å. The values of $d$ for the five remaining $\gamma$-H atoms are much larger: 3.90, 3.90, 4.64, 4.92 and 5.01 Å, which precludes the participation of these atoms in the Yang photocyclization.

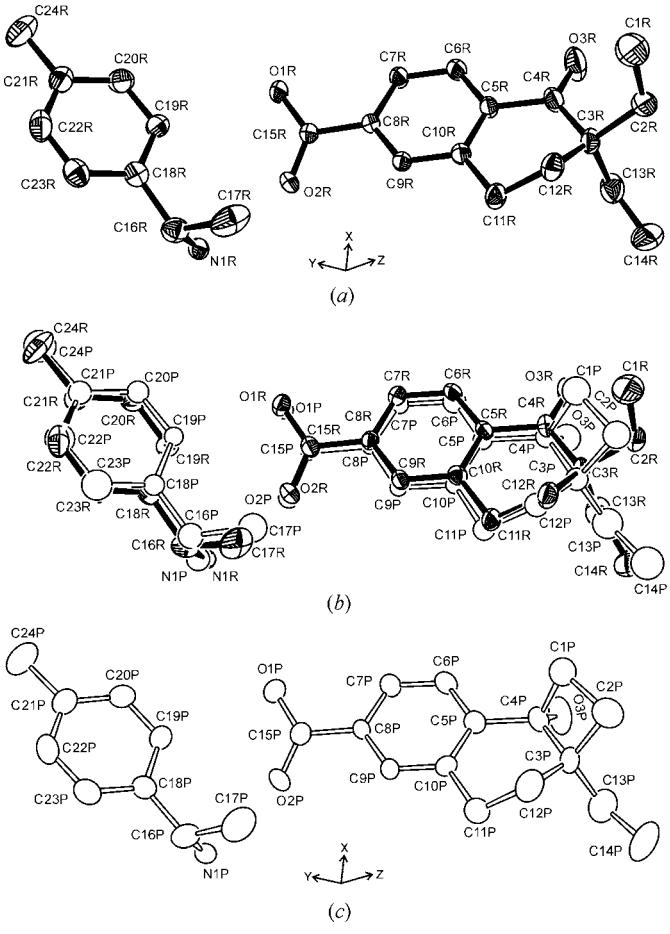


**Figure 1**
*ORTEP* (Farrugia, 1997) view of (*a*) the reactant molecule in the unreacted crystal, (*b*) the product molecule (empty bonds) superimposed on the reactant molecule (filled bonds) for the partly reacted crystal containing 28.6% of the product, and (*c*) the product molecule in the crystal after the photoreaction. H atoms are omitted for clarity. Displacement ellipsoids are drawn at the 20% probability level.

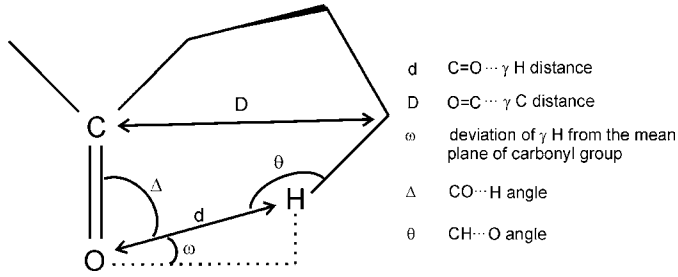


### 3.2. Monitoring the cell constants

Structural changes proceeding in a crystal during a photochemical reaction can be monitored by the cell constants. Fig. 2 presents variations in the cell constants for (1) as a function of irradiation time. As can be seen, $a$ and $b$ increase only slightly, but $c$ shows a large decrease. The change in $c$ is about five times larger than the changes in $a$ and $b$. The most likely reason for such a relation is that the $c$ edge of the unit cell is almost parallel to the direction determined by atoms C1*R* and C4*R*, *i.e.* the atoms which directly take part in the formation of a new bond (see Fig. 1 for atom labels). The value of the angle between the C1*R*–C4*R* line and the $c$ axis is 168.7°, whereas the angles between this line and the $a$ and $b$ edges are close to right angles, and are 100.9 and 87.1°, respectively. However, a similar analysis carried out by us for (2) and (3) revealed that the orientation of the line determined by the reacting C atoms is not the only reason for changes in the cell constants.

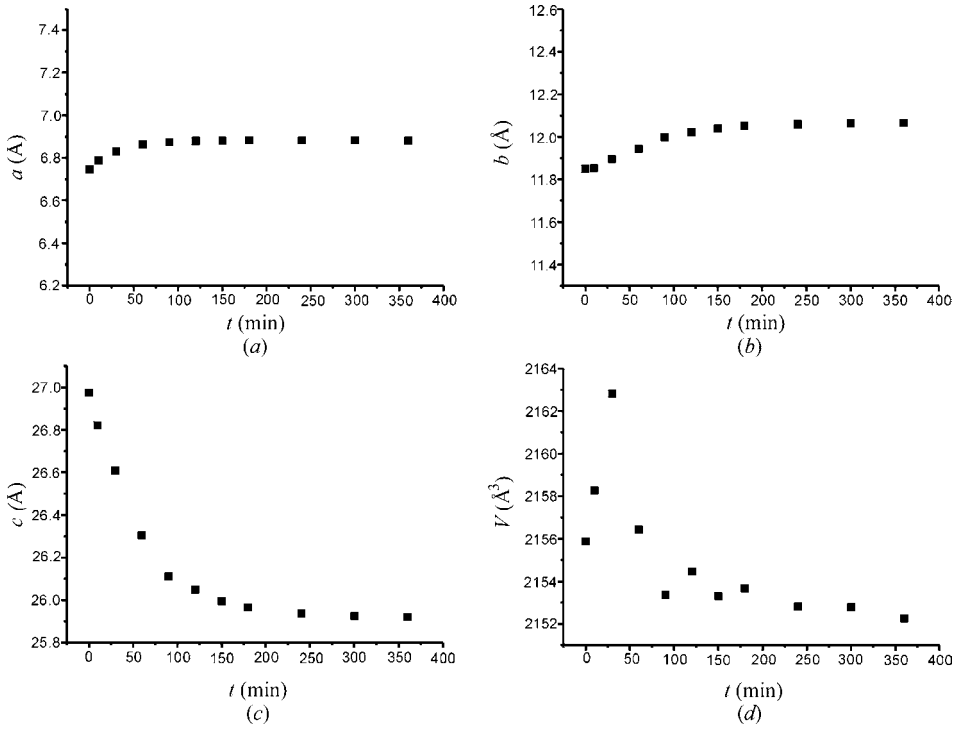


**Figure 2**
Variations in the cell constants and cell volume with time of crystal irradiation. Standard uncertainties for *a*, *b*, *c* and *V* are in the ranges 0.0007–0.0018, 0.0014–0.003, 0.003–0.006 Å, and 0.4–0.9 Å$^3$, respectively.

Variations in the *a*, *b* and *c* parameters are reflected in variations in the cell volume. The cell volume for (1) changes in an interesting manner: at the beginning of the photoreaction it increases and reaches a maximum at 56.5% reaction progress, and afterwards decreases. For the Yang photocyclization of (2) the cell volume reached a maximum at ∼90% reaction progress (Turowska-Tyrk *et al.*, 2006*a*), whereas for the Yang photocyclization of (3) it decreased during the whole reaction (Turowska-Tyrk *et al.*, 2007). In the case of the Yang photocyclization of the 1-(4-carboxybenzoyl)-1-methylnorbornane salt with (*S*)-(−)-1-phenylethylamine, the cell volume increased with the photoreaction progress and was: 2002 (1), 2026.67 (3) and 2053.8 (8) Å$^3$ for 0, 70 and 93% conversion, respectively (Patrick *et al.*, 2003*a*,*b*). It is worth noting that in the case of intermolecular [2 + 2] photocyclization, where a cyclobutane ring is also formed, the cell volume also changes for different compounds in a different way. For 2-benzyl-5-benzylidenecyclopentanone it decreased after an initial small increase (Nakanishi *et al.*, 1980, 1981), for 5-benzylidene-2-(4-chlorobenzyl)cyclopentanone it decreased from the beginning of the photoreaction (Turowska-Tyrk, 2003), and for 5-benzylidene-2-(4-bromobenzyl)cyclopentanone it was constant (Nakanishi *et al.*, 1981).

### 3.3. Monitoring the product content in the crystal

Fig. 3 presents the variation of the product content in the crystal with time of irradiation for (1). As can be seen, the rate of the Yang photocyclization depends on the amount of reactant in the crystal: the less reactant the slower the photoreaction. Similar dependencies were also observed for other intra- (Turowska-Tyrk, Bąkowicz, Scheffer & Xia, 2006; Turowska-Tyrk *et al.*, 2007) and intermolecular photochemical reactions in crystals (Turowska-Tyrk, 2001, 2003; Fernandes & Levendis, 2004).

### 3.4. Monitoring the reaction centre

Fig. 4(*a*) presents the distance between the atoms C1*R* and C4*R*, which directly take part in the Yang photocyclization of (1). As can be seen, these values are ∼3.0 Å. They are statistically constant until about 75% product content in the crystal. Unfortunately, we do not have values for a higher percentage content of the product. For the Yang photocyclization of (2) the distance between directly reacting C atoms was also constant until ∼80% reaction progress, and afterwards it decreased significantly by 0.25 Å (from 2.97 to 2.72 Å; Turowska-Tyrk *et al.*, 2006*a*). It was also constant until about 30% product content, and afterwards decreased, in the case of a retro-Claisen photorearrangement (Turowska-Tyrk, Bąkowicz, Scheffer & Xia, 2006). For the Yang photocyclization of (3) it was impossible to detect a similar decrease because of the lack of experimental data for reaction progress less than 20%. In the case of intermolecular [2 + 2] photocyclizations, directly reacting atoms of neighboring molecules came closer from the beginning of the photoreaction

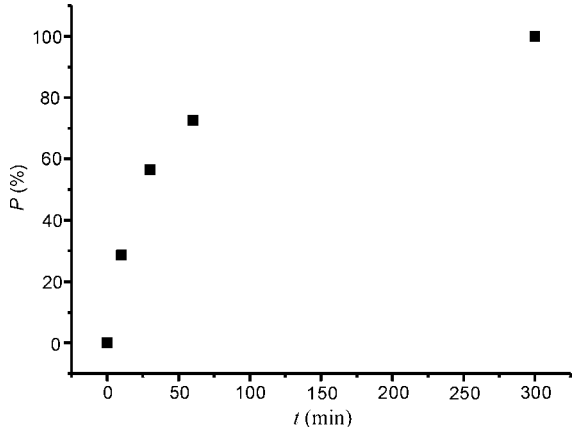


**Figure 3**
Relationship between the product content in the crystal and the time of irradiation. Standard uncertainties for the per cent of the product are in the range 0.0–0.9% with a mean value of 0.5%.

(Turowska-Tyrk, 2003; Turowska-Tyrk & Trzop, 2003). This is understandable since intermolecular distances are more easily changed than intramolecular distances.

Monitoring the distance between directly reacting atoms is very informative. Namely, the distance can determine the direction of a reaction and the type of product obtained (Turowska-Tyrk, Bąkowicz, Scheffer & Xia, 2006). A decrease in distance with the reaction progress was postulated as the reason for the formation of two enantiomorphs during the retro-Claisen photorearrangement in crystals, although the formation of only one enantiomorph was predicted on the basis of the structure of the pure reactant crystal (Turowska-Tyrk, Bąkowicz, Scheffer & Xia, 2006). In the case of (1) we deal with the formation of only one product. In theory, the second enantiomorph could be created as a result of the connecting atoms C4*R* and C14*R* (see Fig. 1 for atom labels), but a geometric analysis rejects the possibility of such a reaction. Namely, the distance between C4*R* and C14*R* is in the range 3.73–3.84 Å during the photoreaction studied, which makes the formation of the second enantiomorph very unlikely (see Table 2 for the average literature value of *D* for compounds undergoing Yang photocyclizations). Moreover, the shortest distance between the carbonyl O3*R* atom and the $\gamma$-H atom at C14*R* is in the range 4.53–4.72 Å during the photoreaction (see Table 2 for the ideal and average values of *d*).

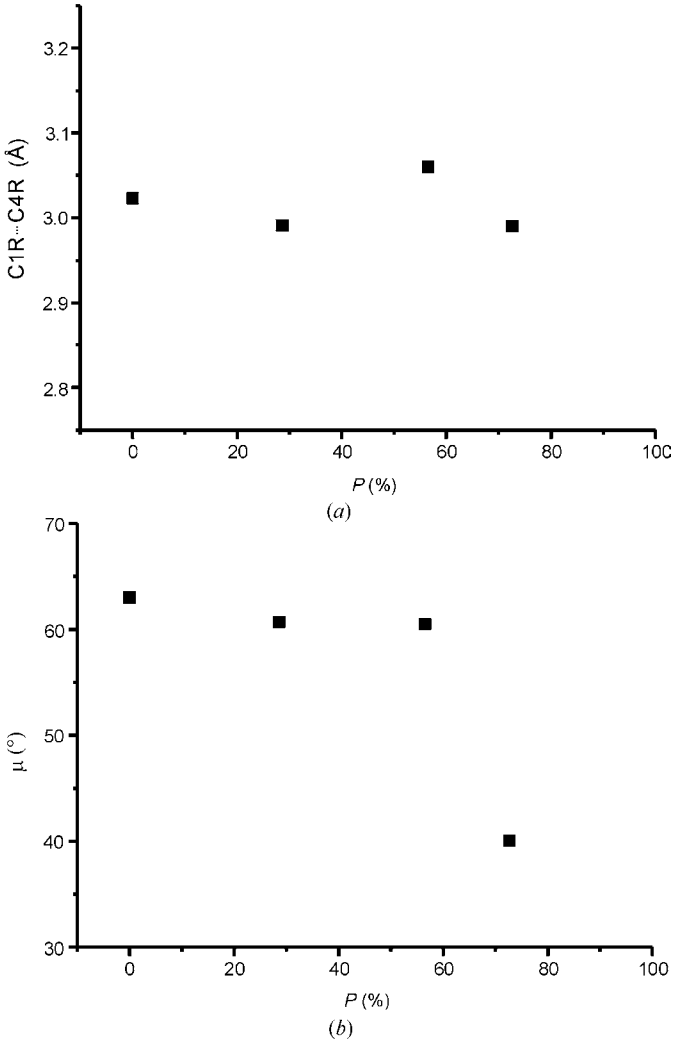


**Figure 4**
Variation in (*a*) the C1*R*···C4*R* distance between directly reacting atoms and (*b*) the C1*R*—C2*R*—C3*R*—C4*R* torsion angle with the product content in the crystal. Standard uncertainties for the distance and for the torsion angle are in the range 0.007–0.03 Å and 0.6–5°, respectively. The largest changes in these parameters are 0.07 (4) Å and 23 (5)°, respectively, which indicates that the distance is statistically constant and the torsion angle is not statistically constant at the 3$\sigma$ level, *i.e.* with 99.7% probability.

During the Yang photocyclization of salt (1) not only the distance between directly reacting C atoms changes, but also their mutual orientation. Fig. 4(*b*) presents a variation in the torsion angle C1*R*—C2*R*—C3*R*—C4*R*. This angle is statistically constant until about 60% photoreaction progress, and afterwards decreases rapidly towards the value observed in the cyclobutane ring in the pure product crystal [15.3 (7)°]. This shows once again that, at a certain reaction stage, reactant molecules start to resemble product molecules, even for intramolecular photoreactions (Turowska-Tyrk *et al.*, 2006*a*). This rapid decrease can be one of the factors influencing the decrease of the cell volume observed after $\sim$60% photoreaction progress (see Fig. 2*d*).

### 3.5. Monitoring movements of molecules

Knowledge of crystal structures for several steps of the photoreaction also enables a description of the changes in positions of molecules in the crystal. Our previous results, both on intra- and intermolecular reactions (Turowska-Tyrk, 2001, 2003; Turowska-Tyrk & Trzop, 2003; Turowska-Tyrk, Bąkowicz, Scheffer & Xia, 2006; Turowska-Tyrk *et al.*, 2006*a*, 2007), revealed that reactant and product molecules did not assume a constant position during the phototransformations and the molecular movements possessed a rotational component. Similar behavior was also observed for (1). Examples of the variations in orientations of several molecular fragments in relation to the *xy* plane are given in the supplementary material.[2] Changes are also observed for the *xz* and *yz* planes. They are smooth in most cases. The greatest change is observed for the $COO^-$ group in reactant molecules: 17.8°. This can be easily understood since $COO^-$ can move around the adjacent C—C bond. However, this rotation is limited by hydrogen bonds in which this group takes part. A change in the orientation of the benzene ring is smaller than for the $COO^-$ group. This can be rationalized if we take into account that the analyzed ring is part of the larger rigid fragment. In the case of (3), where the benzene ring is not fused to another ring, the change of the ring orientation is greater: 12° for reactant molecules and 10° for product molecules (Turowska-Tyrk *et al.*, 2007). In the case of (3) the greatest change of orientation was also observed for the $COO^-$ group partici-

[2] Supplementary data for this paper are available from the IUCr electronic archives (Reference: BK5065). Services for accessing these data are described at the back of the journal.

**Table 3**
Geometry of strong hydrogen bonds in the crystals of the pure reactant and the pure product (Å, °).

Molecule: R = reactant, P = product.

| Bond | Molecule | $D\cdots A$ | $D$—H | H$\cdots A$ | $\angle DHA$ |
|---|---|---|---|---|---|
| N1—H1d$\cdots$O1$^{i}$ | R | 2.768 (3) | 0.89 | 2.02 | 141.4 |
| | P | 2.934 (5) | 0.89 | 2.26 | 131.8 |
| N1—H1e$\cdots$O2 | R | 2.743 (4) | 0.89 | 1.92 | 153.8 |
| | P | 2.761 (5) | 0.89 | 1.91 | 159.5 |
| N1—H1f$\cdots$O1$^{ii}$ | R | 2.816 (4) | 0.89 | 2.10 | 137.2 |
| | P | 2.772 (5) | 0.89 | 2.02 | 141.4 |

Symmetry codes: (i) $x-1, y, z$; (ii) $x-\frac{1}{2}, -y+\frac{1}{2}, -z$.

pating in strong hydrogen bonds: 22° for reactant molecules and 13° for product molecules. A comparison of the data for (1) with data for other intra- (Turowska-Tyrk *et al.*, 2006*a*, 2007) and intermolecular photoreactions (Turowska-Tyrk, 2001, 2003, 2004; Turowska-Tyrk & Trzop, 2003) shows that the respective changes in the orientation of molecular fragments are of a similar size.

### 3.6. Monitoring hydrogen bonds

Fig. 5 and Table 3 present the strong hydrogen bonds for (1). The hydrogen bonds form ribbons which are not disrupted during the photoreaction. The same phenomenon was also observed in the case of (2) and (3) (Turowska-Tyrk *et al.*, 2006*a*, 2007). Analysis of the crystal structures of (1) shows that the geometry of all the hydrogen bonds changes. These changes reflect small variations in the molecular packing brought about by the formation of new chemical bonds and new molecules in a crystal. For instance: N1$\cdots$O1$^{ii}$, which is almost parallel to the $z$ axis, decreases by 1.6% (see Table 3). This change can be correlated with a decrease in the $c$ cell constant (see Fig. 2). Fig. 6 presents variations in the geometry of the N—H$\cdots$O bond for which the largest changes were

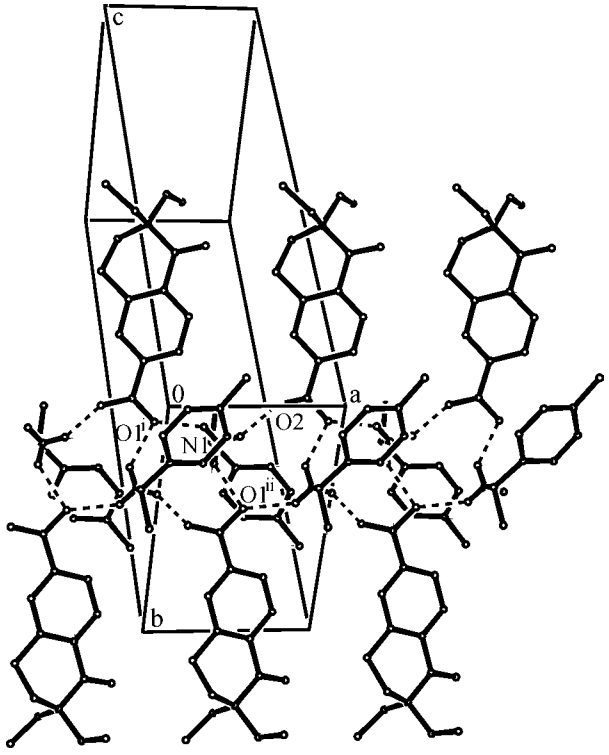


**Figure 5**
Strong hydrogen bonds in the pure reactant crystal.

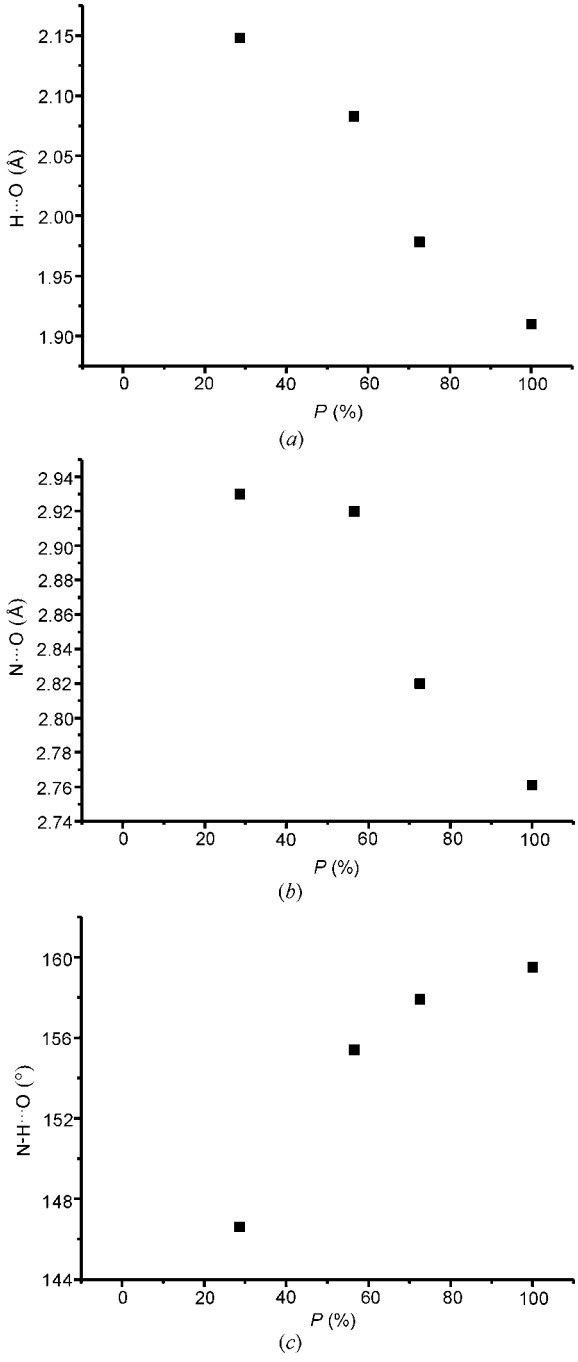


**Figure 6**
Variations in the hydrogen-bond geometry: (*a*) distance H1dP$\cdots$O2P, (*b*) distance N1P$\cdots$O2P and (*c*) angle N1P—H1dP$\cdots$O2P for product molecules during the photoreaction. For N1P$\cdots$O2P standard uncertainties are in the range 0.005–0.04 Å and the change is 0.17 (4) Å, which indicates that it is statistically significant at the 3$\sigma$ level, *i.e.* with 99.7% probability.

observed. As can be seen, the greatest change in distance between the donor and the acceptor is 0.17 Å, and for the hydrogen-bond angle is 13°. A decrease of the distance presented in Fig. 6 is not observed in every case: for some hydrogen bonds the distances decrease and for others they increase. Most of the changes are smooth. In our previous papers on monitoring structural changes in crystals, there was no information about changes in hydrogen bonds. The results reported above for (1) represent the first analysis of this type.

## 4. Conclusions

The structures determined for several steps of the photochemical reaction, *i.e.* for crystals containing the reactant and the product in various proportions, are different. Analysis of intra- and intermolecular geometrical parameters for such crystals provide valuable information on changes in the reaction centre, variations in the orientation of molecular fragments, and changes in intermolecular interactions. A comparison of data for (1) with data for (2) and (3), also undergoing Yang photocyclizations, showed many similarities but also many differences between reaction courses. In the case of (1):

(i) the cell volume increases significantly during the first half of the photoreaction, and afterwards decreases;

(ii) the directly reacting C atoms do not move closer until $\sim 80\%$ photoreaction progress;

(iii) only one enantiomorph is formed in the reaction;

(iv) molecular fragments change their orientation and the greatest variation is observed for the $COO^-$ group;

(v) hydrogen bonds are not disrupted, but their geometry changes during the photoreaction.

## References


Balzani, V. (2003). *Photochem. Photobiol. Sci.* **2**, 459–476.

Boldyreva, E. V. (1999). *Reactivity in Molecular Solids*, edited by E. V. Boldyreva & V. Boldyrev, pp. 1–50. Chichester, New York, Weinheim: Wiley.

Chen, S., Patrick, B. O. & Scheffer, J. R. (2004). *J. Org. Chem.* **69**, 2711–2718.

Cheung, E., Netherton, M. R., Scheffer, J. R. & Trotter, J. (1999). *J. Am. Chem. Soc.* **121**, 2919–2920.

Cohen, M. D. (1975*a*). *Angew. Chem. Int. Ed. Engl.* **14**, 386–393.

Cohen, M. D. (1975*b*). *Angew. Chem.* **87**, 439–447.

Cohen, M. D. & Schmidt, G. M. J. (1964). *J. Chem. Soc.* pp. 1996–2000.

Dürr, H. & Bouas-Laurent, H. (1990). Editors. *Studies in Organic Chemistry: Photochromism Molecules and Systems.* Amsterdam, Oxford, New York, Tokyo: Elsevier.

Enkelman, V., Wegner, G., Novak, K. & Wagener, K. B. (1993). *J. Am. Chem. Soc.* **115**, 10390–10391.

Farrugia, L. J. (1997). *J. Appl. Cryst.* **30**, 565.

Fernandes, M. A. & Levendis, D. C. (2004). *Acta Cryst.* B**60**, 315–324.

Ihmels, H. & Scheffer, J. R. (1999). *Tetrahedron*, **55**, 885–907.

Irie, M. (2000). Editor. *Chem. Rev.* **100**, 1683–1890.

Lavy, T., Sheynin, Y. & Kaftory, M. (2004). *Eur. J. Org. Chem.* pp. 4802–4808.

Nakanishi, H., Jones, W., Thomas, J. M., Hursthouse, M. B. & Motevalli, J. M. (1980). *J. Chem. Soc. Chem. Commun.* pp. 611–612.

Nakanishi, H., Jones, W., Thomas, J. M., Hursthouse, M. B. & Motevalli, J. M. (1981). *J. Phys. Chem.* **85**, 3636–3642.

Natarajan, A., Mague, J. T. & Ramamurthy, V. (2005). *J. Am. Chem. Soc.* **127**, 3568–3576.

Novak, K., Enkelmann, V., Wegner, G. & Wagener, K. B. (1993*a*). *Angew. Chem. Int. Ed. Engl.* **32**, 1614–1616.

Novak, K., Enkelmann, V., Wegner, G. & Wagener, K. B. (1993*b*). *Angew. Chem.* **105**, 1678–1680.

Ohashi, Y. (1988). *Acc. Chem. Res.* **21**, 268–274.

Ohashi, Y. (1993). Editor. *Reactivity in Molecular Crystals.* Tokyo: VCH.

Ohashi, Y. (1998). *Crystalline-State Reactions of Cobaloxime Complexes.* Tokyo Institute of Technology.

Ohba, S. & Ito, Y. (2003). *Acta Cryst.* B**59**, 149–155.

Oxford Diffraction (2003). *Xcalibur CCD CrysAlis*, Version 1.170. Oxford Diffraction Ltd, Wrocław, Poland.

Patrick, B. O., Scheffer, J. R. & Scott, C. (2003*a*). *Angew. Chem. Int. Ed.* **42**, 3775–3777.

Patrick, B. O., Scheffer, J. R. & Scott, C. (2003*b*). *Angew. Chem.* **115**, 3905–3907.

Ramamurthy, V. (1991). *Photochemistry in Organized and Constrained Media*, edited by V. Ramamurthy. New York: VCH.

Scheidt, W. R. & Turowska-Tyrk, I. (1994). *Inorg. Chem.* **33**, 1314–1318.

Schmidt, G. M. J. (1971). *Pure Appl. Chem.* **27**, 647–677.

Sheldrick, G. M. (1990). *Acta Cryst.* A**46**, 467–473.

Sheldrick, G. M. (1997). *SHELX*97. University of Göttingen, Germany.

Tanaka, K. (2003). *Solvent-Free Organic Synthesis.* Weinheim: Wiley-VCH.

Turowska-Tyrk, I. (2001). *Chem. Eur. J.* **7**, 3401–3405.

Turowska-Tyrk, I. (2003). *Acta Cryst.* B**59**, 670–675.

Turowska-Tyrk, I. (2004). *J. Phys. Org. Chem.* **17**, 837–847.

Turowska-Tyrk, I., Bąkowicz, J., Scheffer, J. R. & Xia, W. (2006). *CrystEngComm*, **8**, 616–621.

Turowska-Tyrk, I., Łabęcka, I., Scheffer, J. R. & Xia, W. (2007). *Pol. J. Chem.* **81**, 813–824.

Turowska-Tyrk, I. & Trzop, E. (2003). *Acta Cryst.* B**59**, 779–786.

Turowska-Tyrk, I., Trzop, E., Scheffer, J. R. & Chen, S. (2006*a*). *Acta Cryst.* B**62**, 128–134.

Turowska-Tyrk, I., Trzop, E., Scheffer, J. R. & Chen, S. (2006*b*). *IUCr Newsl.* **14**, 4.

Weiss, R. G., Ramamurthy, V. & Hammond, G. (1993). *Acc. Chem. Res.* **26**, 530–536.

Xia, W., Scheffer, J. R., Botoshansky, M. & Kaftory, M. (2005). *Org. Lett.* **7**, 1315–1318.

Yang, C., Xia, W., Scheffer, J. R., Botoshansky, M. & Kaftory, M. (2005*a*). *Angew. Chem. Int. Ed.* **44**, 5087–5089.

Yang, C., Xia, W., Scheffer, J. R., Botoshansky, M. & Kaftory, M. (2005*b*). *Angew. Chem.* **117**, 5217–5219.